



Available online at <http://scik.org>

Commun. Math. Biol. Neurosci. 2022, 2022:27

<https://doi.org/10.28919/cmbn/7236>

ISSN: 2052-2541

MULTISTAGE VARIATIONAL ITERATION METHOD FOR A SEIQR COVID-19 EPIDEMIC MODEL WITH ISOLATION CLASS

IFFAH NURIL KHASANAH, AGUS SURYANTO*, UMMU HABIBAH

Department of Mathematics, Faculty of Mathematics and Natural Sciences, University of Brawijaya, Jl. Veteran,
Malang 65145, Indonesia

Copyright © 2022 the author(s). This is an open access article distributed under the Creative Commons Attribution License, which permits unrestricted use, distribution, and reproduction in any medium, provided the original work is properly cited.

Abstract. The SEIQR COVID-19 epidemic model is in the form of the system of first-order nonlinear differential equations. In this paper we propose multistage versions of the variational iteration method (VIM) to solve this COVID-19 epidemic model. The idea of multistage version is to divide the entire time domain into a finite number of subintervals and then implementing the VIM piecewisely on each subinterval. There are two kinds of multistage methods discussed in this paper, where the difference between the two methods lies in the number of restricted variations used in the correction functional. The multistage methods generally give more accurate solutions on longer time intervals than the classical versions. The multistage VIM with less number of restricted variations has the best performance among all types of variational iteration methods discussed in this paper. The accuracy of multistage VIM solution can be increased by using smaller size of subinterval or by implementing more iterations in each subinterval.

Keywords: COVID-19 epidemic model; SEIQR epidemic model; analytical approximation method; multistage variational iteration method.

2010 AMS Subject Classification: 34A34, 47J30, 92D30.

*Corresponding author

E-mail address: suryanto@ub.ac.id

Received February 06, 2022

1. INTRODUCTION

Recently, we are facing the pandemic of COVID-19, an infectious disease caused by new type of corona virus (SARS-CoV-2) that infects respiratory system. Common symptoms of this virus are fever, fatigue, dry cough, throat infection, as well as anosmia [1]. In 2020, COVID-19 spreads to various countries causing a deadly pandemic. The COVID-19 pandemic has had a devastating impact on the health, economic, as well as social sectors around the world.

Mathematical epidemic modeling is one way to understand the spread of infectious disease. There are two classes of mathematical epidemic model. The first class is phenomenological model which is an empirical model without any biological mechanism assumption. The phenomenological model has been applied to COVID-19 data, see for example [2, 3, 4, 5]. The second class is mechanistic compartment model. In this model, the population is divided into some subpopulations which correspond to the health states. For example, Kermack and McKendrick [6] introduced a SIR (Susceptible Infective Removal) epidemic model. The SIR model describes a disease spread into susceptible individuals whom can be infected through the process of interaction between the infected and the recovered individuals. The researchers create more specific epidemic models using the SIR model as the basic model. Zeb et al. [7] described the spread of COVID-19 using the SEIQR model. The populations were divided into five subpopulations, namely susceptible, exposed, infected, isolated, and recovered. The increasing of infected COVID-19 subpopulation is mainly caused by contact between susceptible individuals with exposed or infected individuals. Therefore, isolation of both exposed and infected individuals is carried out to reduce the risk of COVID-19 spread. Isolation class are therefore added to the model. Based on these assumptions, Zeb et al. [7] derived a mathematical model which describes the spread of COVID-19. In the normalized variables, this model is given by the following system of differential equations.

TABLE 1. Description of parameters.

Parameter	Description
α	Recruitment rate
β	Rate at which susceptible individuals moves to exposed class
π	Rate at which exposed individuals become infected
γ	Rate at which exposed individuals move to isolation class
σ	Rate at which infected individuals move to isolation class
θ	Rate at which isolated individuals become recovered
μ	Death rate

$$\begin{aligned}
(1) \quad \frac{dv(t)}{dt} &= \mu - \mu v(t) - \beta \frac{\alpha}{\mu} v(t)(w(t) + x(t)), \\
\frac{dw(t)}{dt} &= \beta \frac{\alpha}{\mu} v(t)(w(t) + x(t)) - (\pi + \mu + \gamma)w(t), \\
\frac{dx(t)}{dt} &= \pi w(t) - (\sigma + \mu)x(t), \\
\frac{dy(t)}{dt} &= \gamma w(t) + \sigma x(t) - (\theta + \mu)y(t), \\
\frac{dz(t)}{dt} &= \theta y(t) - \mu z(t),
\end{aligned}$$

where $v(t), w(t), x(t), y(t)$, and $z(t)$ are respectively the normalized susceptible subpopulation, exposed subpopulation, infected subpopulation, isolated subpopulation and recovered subpopulation. All parameters in the system (1) are positive and are described in Table 1. Since the equation for variable $z(t)$ in the system (1) does not depend on any other variables, we only focus on the first four equations with initial condition

$$(2) \quad v(0) = v_0 \geq 0, w(0) = w_0 \geq 0, x(0) = x_0 \geq 0, \text{ and } y(0) = y_0 \geq 0.$$

The COVID-19 epidemic model (1) is in the form of system of first-order differential equations. Unfortunately, such system of differential equations as well as almost all epidemic models are nonlinear. Exact solutions to nonlinear differential equations are generally not available and difficult to find. There are many techniques to determine the approximate solutions. Some

analytical approximation methods to get solutions of the system of first-order nonlinear differential equations are adomian decomposition method (ADM) [8], homotopy perturbation method (HPM) [9, 10], and variational iteration method (VIM) [11, 12, 13]. Recently, Trisilowati et al. [14] have implemented the VIM to solve the system (1). Firstly they applied restricted variations for both linear and nonlinear terms in the correction functional and showed that the solution obtained by such VIM is accurate only in the vicinity of the initial value. Then they improved the VIM by reducing the number of restricted variations. The improved variational iteration method (IVIM) gave approximate solutions that are efficient for a larger interval. However, the IVIM cannot be applied for problem with much larger intervals. Hence, in this paper we propose multistage version of both VIM and IVIM to solve the COVID-19 epidemic model (1). As introduced in [15, 16, 17], the idea of multistage variational iteration method (MVIM) and multistage improved variational iteration method (MIVIM) is to divide the entire time domain into a finite number of subintervals and then implementing the VIM or IVIM piecewisely on each subinterval.

This paper is organized as follows. In Section 2 we review VIM and IVIM proposed by Trisilowati et al. [14]. The proposed MVIM and MIVIM for the COVID-19 epidemic model (1) are presented in Section 3. The numerical examples and discussion are given in Section 4. Finally we provide a brief conclusion in Section 5.

2. VARIATIONAL ITERATION METHOD (VIM)

The variational iteration method was introduced by He [12] to solve differential equations. The first step in the variational iteration method is to express the nonlinear differential equation in an operator form. For a system of m differential equations, the operator form is denoted by

$$(3) \quad \mathcal{L}u_i(t) + \mathcal{N}u_i(t) = g_i(t), \quad i = 1, 2, \dots, m$$

where \mathcal{L} is a linear operator, \mathcal{N} is a nonlinear operator, and $g_i(t)$ are non-homogeneous terms.

The sequence of $u_i(t)$ is made in such a way that it approximates the exact solution of the model. The $u_i(t)$ component can be calculated by the following correction functional:

$$(4) \quad u_{i,n+1}(t) = u_{i,n}(t) + \int_0^t \lambda (\mathcal{L}u_{i,n}(\tau) + \mathcal{N}\tilde{u}_{i,n}(\tau) - g_i(\tau)) d\tau,$$

where λ is a Lagrange multiplier, which can be optimally identified through the variational theory. Index n denotes the n -th iteration, \tilde{u} denotes restricted variation so that $\delta\tilde{u} = 0$. Once the Lagrange multiplier is identified, iteration (4) can be operated using the initial value.

In many implementations, the correction functional (4) is applied by considering the restricted variations for both linear and nonlinear terms. For example, Trisilowati et al. [14] have applied this approach to the system (1) with initial condition (2) to get the following correction functional

$$\begin{aligned}
v_{n+1}(t) &= v_n(t) + \int_0^t \lambda_1(\tau) \left[\frac{dv_n(\tau)}{d\tau} - \mu + \mu \tilde{v}_n(\tau) + \beta \frac{\alpha}{\mu} \tilde{v}_n(\tau) (\tilde{w}_n(\tau) + \tilde{x}_n(\tau)) \right] d\tau, \\
w_{n+1}(t) &= w_n(t) + \int_0^t \lambda_2(\tau) \left[\frac{dw_n(\tau)}{d\tau} - \beta \frac{\alpha}{\mu} \tilde{v}_n(\tau) (\tilde{w}_n(\tau) + \tilde{x}_n(\tau)) \right] d\tau \\
(5) \quad &+ \int_0^t \lambda_2(\tau) \left[(\pi + \mu + \gamma) \tilde{w}_n(\tau) \right] d\tau, \\
x_{n+1}(t) &= x_n(t) + \int_0^t \lambda_3(\tau) \left[\frac{dx_n(\tau)}{d\tau} - \pi \tilde{w}_n(\tau) + (\sigma + \mu) \tilde{x}_n(\tau) \right] d\tau, \\
y_{n+1}(t) &= y_n(t) + \int_0^t \lambda_4(\tau) \left[\frac{dy_n(\tau)}{d\tau} - \gamma \tilde{w}_n(\tau) - \sigma \tilde{x}_n(\tau) + (\theta + \mu) \tilde{y}_n(\tau) \right] d\tau.
\end{aligned}$$

The optimality condition for this case leads to the Lagrange multipliers $\lambda = -1$ for all equations and the variational iteration method (VIM) for system (1) is given by the following system (see [14] for the detail)

$$\begin{aligned}
v_{n+1}(t) &= v_n(t) - \int_0^t \left[\frac{dv_n(\tau)}{d\tau} - \mu + \mu v_n(\tau) + \beta \frac{\alpha}{\mu} v_n(\tau) (w_n(\tau) + x_n(\tau)) \right] d\tau, \\
w_{n+1}(t) &= w_n(t) - \int_0^t \left[\frac{dw_n(\tau)}{d\tau} - \beta \frac{\alpha}{\mu} v_n(\tau) (w_n(\tau) + x_n(\tau)) + (\pi + \mu + \gamma) w_n(\tau) \right] d\tau, \\
(6) \quad x_{n+1}(t) &= x_n(t) - \int_0^t \left[\frac{dx_n(\tau)}{d\tau} - \pi w_n(\tau) + (\sigma + \mu) x_n(\tau) \right] d\tau, \\
y_{n+1}(t) &= y_n(t) - \int_0^t \left[\frac{dy_n(\tau)}{d\tau} - \gamma w_n(\tau) - \sigma x_n(\tau) + (\theta + \mu) y_n(\tau) \right] d\tau,
\end{aligned}$$

where $n = 0, 1, 2, \dots$.

Trisilowati et al. [14] have improved the VIM (6) by reducing the restriction variations in the correction functionals as follows

$$\begin{aligned}
v_{n+1}(t) &= v_n(t) + \int_0^t \lambda_1(\tau) \left[\frac{dv_n(\tau)}{d\tau} - \mu + \mu v_n(\tau) + \beta \frac{\alpha}{\mu} \tilde{v}_n(\tau) (\tilde{w}_n(\tau) + \tilde{x}_n(\tau)) \right] d\tau, \\
w_{n+1}(t) &= w_n(t) + \int_0^t \lambda_2(\tau) \left[\frac{dw_n(\tau)}{d\tau} - \beta \frac{\alpha}{\mu} \tilde{v}_n(\tau) (\tilde{w}_n(\tau) + \tilde{x}_n(\tau)) \right] d\tau \\
&\quad + \int_0^t \lambda_2(\tau) \left[(\pi + \mu + \gamma) w_n(\tau) \right] d\tau, \\
x_{n+1}(t) &= x_n(t) + \int_0^t \lambda_3(\tau) \left[\frac{dx_n(\tau)}{d\tau} - \pi \tilde{w}_n(\tau) + (\sigma + \mu) x_n(\tau) \right] d\tau, \\
y_{n+1}(t) &= y_n(t) + \int_0^t \lambda_4(\tau) \left[\frac{dy_n(\tau)}{d\tau} - \gamma \tilde{w}_n(\tau) - \sigma \tilde{x}_n(\tau) + (\theta + \mu) y_n(\tau) \right] d\tau.
\end{aligned}
\tag{7}$$

The Lagrange multipliers for the variational iteration (7) are identified as follows

$$\begin{aligned}
\lambda_1 &= -e^{\mu(\tau-t)}, \\
\lambda_2 &= -e^{(\pi+\mu+\gamma)(\tau-t)}, \\
\lambda_3 &= -e^{(\sigma+\mu)(\tau-t)}, \\
\lambda_4 &= -e^{(\theta+\mu)(\tau-t)}.
\end{aligned}
\tag{8}$$

Thus, the improved variational iteration method (IVIM) for system (1) can be written as

$$\begin{aligned}
v_{n+1}(t) &= v_n(t) - \int_0^t e^{\mu(\tau-t)} \left[\frac{dv_n(\tau)}{d\tau} - \mu + \mu v_n(\tau) + \beta \frac{\alpha}{\mu} v_n(\tau) (w_n(\tau) + x_n(\tau)) \right] d\tau, \\
w_{n+1}(t) &= w_n(t) - \int_0^t e^{(\pi+\mu+\gamma)(\tau-t)} \left[\frac{dw_n(\tau)}{d\tau} - \beta \frac{\alpha}{\mu} v_n(\tau) (w_n(\tau) + x_n(\tau)) \right] d\tau \\
&\quad - \int_0^t e^{(\pi+\mu+\gamma)(\tau-t)} \left[(\pi + \mu + \gamma) w_n(\tau) \right] d\tau, \\
x_{n+1}(t) &= x_n(t) - \int_0^t e^{(\sigma+\mu)(\tau-t)} \left[\frac{dx_n(\tau)}{d\tau} - \pi w_n(\tau) + (\sigma + \mu) x_n(\tau) \right] d\tau, \\
y_{n+1}(t) &= y_n(t) - \int_0^t e^{(\theta+\mu)(\tau-t)} \left[\frac{dy_n(\tau)}{d\tau} - \gamma w_n(\tau) - \sigma x_n(\tau) + (\theta + \mu) y_n(\tau) \right] d\tau,
\end{aligned}
\tag{9}$$

where $n = 0, 1, 2, \dots$, see [14] for the detail.

3. MULTISTAGE VARIATIONAL ITERATION METHOD

We notice that the correction functionals for both VIM or IVIM, see respectively (5) and (7), are defined for the entire domain $[0, T]$. Thus, the resulting iterative formulas VIM (6) and IVIM (9) can be implemented for all $t \in [0, T]$. It has been shown by Trisilowati et al. [14] that

the IVIM (9) has improved the performance of the VIM (6). In this case, the solution obtained by the IVIM is reliable for longer time domain than that obtained by the VIM. However, as we see in the next section, the solution obtained by the IVIM also becomes inaccurate for much larger time domain. To overcome this problem, we consider a modified version of both VIM and IVIM, namely the multistage variational iteration method (MVIM) and the multistage improved variational iteration method (MIVIM). To construct the MVIM and MIVIM, domain $I = [0, T]$ is divided into M uniform subintervals $I_j = [t_{j-1}, t_j]$ with $j = 1, 2, \dots, M$, $t_0 = 0$, and $t_M = T$. Each subinterval has the same length $\Delta t = t_j - t_{j-1}$ for each j . Then, by following Geng et al. [16] and Goh et al. [17], the correction functional of MVIM is defined for each subinterval $I_j, j = 1, 2, \dots, M$ as follows

(10)

$$\begin{aligned}
v_{j,n+1}(t) &= v_{j,n}(t) + \int_{t_{j-1}}^t \lambda_1(\tau) \left[\frac{dv_{j,n}(\tau)}{d\tau} - \mu + \mu \tilde{v}_{j,n}(\tau) + \beta \frac{\alpha}{\mu} \tilde{v}_{j,n}(\tau) (\tilde{w}_{j,n}(\tau) + \tilde{x}_{j,n}(\tau)) \right] d\tau, \\
w_{j,n+1}(t) &= w_{j,n}(t) + \int_{t_{j-1}}^t \lambda_2(\tau) \left[\frac{dw_{j,n}(\tau)}{d\tau} - \beta \frac{\alpha}{\mu} \tilde{v}_{j,n}(\tau) (\tilde{w}_{j,n}(\tau) + \tilde{x}_{j,n}(\tau)) \right] d\tau \\
&\quad + \int_{t_{j-1}}^t \lambda_2(\tau) \left[(\pi + \mu + \gamma) \tilde{w}_{j,n}(\tau) \right] d\tau, \\
x_{j,n+1}(t) &= x_{j,n}(t) + \int_{t_{j-1}}^t \lambda_3(\tau) \left[\frac{dx_{j,n}(\tau)}{d\tau} - \pi \tilde{w}_{j,n}(\tau) + (\sigma + \mu) \tilde{x}_{j,n}(\tau) \right] d\tau, \\
y_{j,n+1}(t) &= y_{j,n}(t) + \int_{t_{j-1}}^t \lambda_4(\tau) \left[\frac{dy_{j,n}(\tau)}{d\tau} - \gamma \tilde{w}_{j,n}(\tau) - \sigma \tilde{x}_{j,n}(\tau) + (\theta + \mu) \tilde{y}_{j,n}(\tau) \right] d\tau
\end{aligned}$$

for $t_{j-1} \leq t \leq t_j$. As noticed by Goh et al. [17], $\delta v_{j,n}(t_{j-1}) = \delta w_{j,n}(t_{j-1}) = \delta x_{j,n}(t_{j-1}) = \delta y_{j,n}(t_{j-1}) = 0$, and hence the Lagrange multipliers can be determined as in the case of VIM, which in this case are also identified as $\lambda_i = -1, i = 1, 2, 3, 4$. The MVIM for system (1) is then given by the following set of iterative formulae

(11)

$$\begin{aligned}
v_{j,n+1}(t) &= v_{j,n}(t) - \int_{t_{j-1}}^t \left[\frac{dv_{j,n}(\tau)}{d\tau} - \mu + \mu v_{j,n}(\tau) + \beta \frac{\alpha}{\mu} v_{j,n}(\tau) (w_{j,n}(\tau) + x_{j,n}(\tau)) \right] d\tau, \\
w_{j,n+1}(t) &= w_{j,n}(t) - \int_{t_{j-1}}^t \left[\frac{dw_{j,n}(\tau)}{d\tau} - \beta \frac{\alpha}{\mu} v_{j,n}(\tau) (w_{j,n}(\tau) + x_{j,n}(\tau)) + (\pi + \mu + \gamma) w_{j,n}(\tau) \right] d\tau, \\
x_{j,n+1}(t) &= x_{j,n}(t) - \int_{t_{j-1}}^t \left[\frac{dx_{j,n}(\tau)}{d\tau} - \pi w_{j,n}(\tau) + (\sigma + \mu) x_{j,n}(\tau) \right] d\tau,
\end{aligned}$$

$$y_{j,n+1}(t) = y_{j,n}(t) - \int_{t_{j-1}}^t \left[\frac{dy_{j,n}(\tau)}{d\tau} - \gamma w_{j,n}(\tau) - \sigma x_{j,n}(\tau) + (\theta + \mu)y_{j,n}(\tau) \right] d\tau,$$

where $n = 0, 1, 2, \dots$. As is well known, if we take more number of iteration steps then we should get more accurate solutions. Suppose for each subinterval we iterate until $n = n_1$. The initial value for the first subinterval is $v_{1,0} = v(0), w_{1,0} = w(0), x_{1,0} = x(0), y_{1,0} = y(0)$, while for subinterval $I_j, j = 2, 3, \dots, M$, the initial values are given by

$$(12) \quad \begin{aligned} v_{j,0}(t_{j-1}) &= v_{j-1,n_1}(t_{j-1}), \\ w_{j,0}(t_{j-1}) &= w_{j-1,n_1}(t_{j-1}), \\ x_{j,0}(t_{j-1}) &= x_{j-1,n_1}(t_{j-1}), \\ y_{j,0}(t_{j-1}) &= y_{j-1,n_1}(t_{j-1}). \end{aligned}$$

Based on the correction functional (7) and applying the same procedure as for the MVIM, we obtain the following MIVIM for system (1)

$$(13) \quad \begin{aligned} v_{j,n+1}(t) &= v_{j,n}(t) - \int_{t_{j-1}}^t e^{\mu(\tau-t)} \left[\frac{dv_{j,n}(\tau)}{d\tau} - \mu + \mu v_{j,n}(\tau) + \beta \frac{\alpha}{\mu} v_{j,n}(\tau) (w_{j,n}(\tau) + x_{j,n}(\tau)) \right] d\tau, \\ w_{j,n+1}(t) &= w_{j,n}(t) - \int_{t_{j-1}}^t e^{(\pi+\mu+\gamma)(\tau-t)} \left[\frac{dw_{j,n}(\tau)}{d\tau} - \beta \frac{\alpha}{\mu} v_{j,n}(\tau) (w_{j,n}(\tau) + x_{j,n}(\tau)) \right] d\tau \\ &\quad - \int_{t_{j-1}}^t e^{(\pi+\mu+\gamma)(\tau-t)} \left[(\pi + \mu + \gamma) w_{j,n}(\tau) \right] d\tau, \\ x_{j,n+1}(t) &= x_{j,n}(t) - \int_{t_{j-1}}^t e^{(\sigma+\mu)(\tau-t)} \left[\frac{dx_{j,n}(\tau)}{d\tau} - \pi w_{j,n}(\tau) + (\sigma + \mu) x_{j,n}(\tau) \right] d\tau, \\ y_{j,n+1}(t) &= y_{j,n}(t) - \int_{t_{j-1}}^t e^{(\theta+\mu)(\tau-t)} \left[\frac{dy_{j,n}(\tau)}{d\tau} - \gamma w_{j,n}(\tau) - \sigma x_{j,n}(\tau) + (\theta + \mu) y_{j,n}(\tau) \right] d\tau, \end{aligned}$$

for $j = 1, 2, \dots, M$ and $n = 0, 1, 2, \dots$; subject to initial values (12).

4. NUMERICAL EXAMPLES AND DISCUSSION

The integrals in the iterative forms of VIM (6), IVIM (9), MVIM (11) and MIVIM (13) can be calculated exactly by computer algebra such as MAPLE software. For example, Trisilowati et al [14] have implemented iterative formulas VIM (6) and IVIM (9) to solve system (1) with

parameter values

$$(14) \quad \alpha = \frac{28}{100}, \beta = \frac{1}{2}, \phi = \frac{3}{10}, \gamma = \frac{8}{100}, \sigma = \frac{2}{10}, \theta = \frac{1}{10}, \mu = \frac{3}{10},$$

and initial value

$$(15) \quad v_0 = \frac{1}{10}, w_0 = \frac{3}{10}, x_0 = \frac{2}{10}, y_0 = \frac{4}{10}.$$

The first and second iterations of VIM (6) produce solutions as follows:

(1) *The first iteration of (VIM)*

$$\begin{aligned} v_1^{VIM}(t) &= \frac{1}{10} + \frac{37}{150}t, \\ w_1^{VIM}(t) &= \frac{3}{10} - \frac{271}{1500}t, \\ x_1^{VIM}(t) &= \frac{1}{5} - \frac{1}{100}t, \\ y_1^{VIM}(t) &= \frac{2}{5} - \frac{12}{125}t, \end{aligned}$$

(2) *The second iteration of VIM*

$$\begin{aligned} v_2^{VIM}(t) &= \frac{1}{10} + \frac{37}{150}t - \frac{13799}{225000}t^2 + \frac{37037}{5062500}t^3, \\ w_2^{VIM}(t) &= \frac{3}{10} - \frac{271}{1500}t + \frac{3859}{45000}t^2 - \frac{37037}{5062500}t^3, \\ x_2^{VIM}(t) &= \frac{1}{5} - \frac{1}{100}t - \frac{123}{5000}t^2, \\ y_2^{VIM}(t) &= \frac{2}{5} - \frac{12}{125}t + \frac{823}{75000}t^2. \end{aligned}$$

Furthermore, the first and second iterations of IVIM (9) give the following results:

(1) *The first iteration of IVIM*

$$\begin{aligned} v_1^{IVIM}(t) &= \frac{83}{90} - \frac{37}{45}e^{-\frac{3}{10}t}, \\ w_1^{IVIM}(t) &= \frac{7}{204} + \frac{271}{1020}e^{-\frac{17}{25}t}, \\ x_1^{IVIM}(t) &= \frac{9}{50} + \frac{1}{50}e^{-\frac{1}{2}t}, \\ y_1^{IVIM}(t) &= \frac{4}{25} + \frac{6}{25}e^{-\frac{2}{5}t}, \end{aligned}$$

(2) *The second iteration of IVIM*

$$\begin{aligned}
v_2^{IVIM}(t) &= \frac{1430467}{2065500} - \frac{1286321783}{1667891250}e^{-\frac{3}{10}t} + \frac{157451}{523260}e^{-\frac{17}{25}t} + \frac{581}{13500}e^{-\frac{1}{2}t} + \frac{283087}{3442500}e^{-\frac{3}{10}t} \\
&\quad - \frac{70189}{468180}e^{-\frac{49}{50}t} - \frac{259}{16875}e^{-\frac{4}{5}t}, \\
w_2^{IVIM}(t) &= \frac{635033}{4681800} - \frac{18899653}{266862600}e^{-\frac{17}{25}t} + \frac{157451}{1377000}e^{-\frac{17}{25}t} + \frac{581}{12150}e^{-\frac{1}{2}t} - \frac{283087}{1308150}e^{-\frac{3}{10}t} \\
&\quad + \frac{70189}{206550}e^{-\frac{49}{50}t} + \frac{259}{4050}e^{-\frac{4}{5}t}, \\
x_2^{IVIM}(t) &= \frac{7}{340} + \frac{28}{45}e^{-\frac{1}{2}t} - \frac{271}{612}e^{-\frac{17}{25}t}, \\
y_2^{IVIM}(t) &= \frac{247}{2550} + \frac{44}{105}e^{-\frac{2}{5}t} - \frac{271}{3570}e^{-\frac{17}{25}t} - \frac{1}{25}e^{-\frac{1}{2}t}.
\end{aligned}$$

The iteration of both VIM and IVIM can be continued to get more accurate solutions.

We now implement the MVIM (11) with parameter values (14) and initial value (15). By taking $\Delta t = 3$ and performing two iterations for each interval, the MVIM solutions for the first and second intervals are given in iteration forms as follows:

(1) *The MVIM solution on subinterval $I_1 = [0, 3]$*

(a) The first iteration solution:

$$\begin{aligned}
v_{1,1}^{MVIM}(t) &= \frac{1}{10} + \frac{37}{150}t, \\
w_{1,1}^{MVIM}(t) &= \frac{3}{10} - \frac{271}{1500}t, \\
x_{1,1}^{MVIM}(t) &= \frac{1}{5} - \frac{1}{100}t, \\
y_{1,1}^{MVIM}(t) &= \frac{2}{5} - \frac{12}{125}t.
\end{aligned}$$

(b) The second iteration solution:

$$\begin{aligned}
v_{1,2}^{MVIM}(t) &= \frac{1}{10} + \frac{37}{150}t - \frac{13799}{225000}t^2 + \frac{37037}{5062500}t^3, \\
w_{1,2}^{MVIM}(t) &= \frac{3}{10} - \frac{271}{1500}t + \frac{3859}{45000}t^2 - \frac{37037}{5062500}t^3, \\
x_{1,2}^{MVIM}(t) &= \frac{1}{5} - \frac{1}{100}t - \frac{123}{5000}t^2, \\
y_{1,2}^{MVIM}(t) &= \frac{2}{5} - \frac{12}{125}t + \frac{823}{75000}t^2.
\end{aligned}$$

(2) *The MVIM solution on subinterval $I_2 = [3, 6]$*

(a) The first iteration solution:

$$\begin{aligned} v_{2,1}^{MVIM}(t) &= \frac{75065252299}{351562500000} + \frac{95643185201}{1054687500000}t, \\ w_{2,1}^{MVIM}(t) &= \frac{287987378951}{351562500000} - \frac{171173941451}{1054687500000}t, \\ x_{2,1}^{MVIM}(t) &= -\frac{133607}{312500} + \frac{78363}{625000}t, \\ y_{2,1}^{MVIM}(t) &= \frac{324037}{781250} - \frac{637523}{9375000}t. \end{aligned}$$

(b) The second iteration solution:

$$\begin{aligned} v_{2,2}^{MVIM}(t) &= 0.06119180166 + 0.1969222813 t - 0.02004986881 t^2 + 0.0005207718727 t^3, \\ w_{2,2}^{MVIM}(t) &= 1.345700623 - 0.5180095513 t + 0.06162868938 t^2 - 0.0005207718727 t^3, \\ x_{2,2}^{MVIM}(t) &= -0.9287518451 + 0.4595204300 t - 0.05568993834 t^2, \\ y_{2,2}^{MVIM}(t) &= 0.5915871240 - 0.1858822960 t + 0.01964664044 t^2. \end{aligned}$$

We remark that the MVIM solution on the first subinterval (I_1) is exactly the same as the solution of VIM. It is also noticed that the initial value for the second subinterval (I_2) is the last iteration solution on the subinterval I_1 evaluated at $t = t_1 = \Delta t$. The same procedure can be continued to get solutions on next subintervals $I_j, j = 2, 3, \dots, M$. As in the case of VIM, the MVIM iteration at each interval can also be carried out further to obtain a more accurate solution.

If we implement the MIVIM (13) with $\Delta t = 3$, then we obtain an iterative solution on subinterval $I_1 = [0, 3]$, which is exactly the same as the IVIM solution. Solutions on successive subintervals $I_j, j = 2, 3, \dots, M$ can be calculated in the same way as for the MVIM. The MIVIM solutions are very long to express and are not shown here.

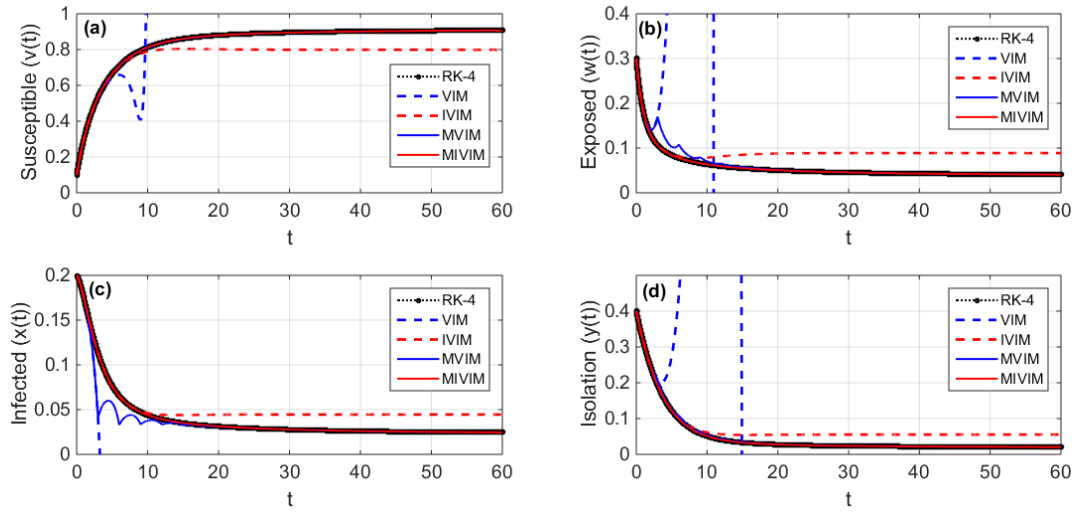


FIGURE 1. Comparison of VIM, IVIM, MVIM and MIVIM solutions on interval $[0.60]$. MVIM and MIVIM solutions are calculated using $\Delta t = 3$.

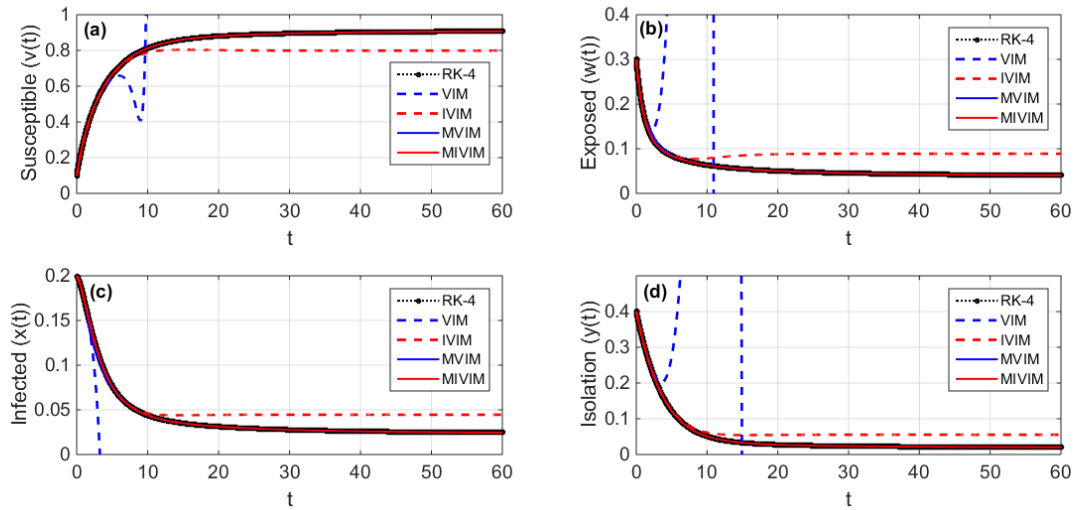


FIGURE 2. Comparison of VIM, IVIM, MVIM and MIVIM solutions on interval $[0.60]$. MVIM and MIVIM solutions are calculated using $\Delta t = 2$.

In Figure 1 and Figure 2 we plot the solutions given by the fourth iteration of VIM (6) and IVIM (9), respectively. For comparison, we also plot the solution obtained by the fourth-order Runge-Kutta method (RK-4) with a very small time step, i.e. $h = 10^{-6}$. Since an exact solution is not available, the RK-4 solution is considered as the reference solution. It is seen that the VIM

solution for all subpopulations ($v(t)$, $w(t)$, $x(t)$, and $y(t)$) is accurate only for t around the initial value. The accuracy of the VIM solution gets worse for larger t . Indeed, the values of these subpopulations are out of bounds, as shown in Figure 1 and Figure 2. As seen in Figure 1 and Figure 2, the IVIM produces a better approximation than the VIM, namely that the approximate solution obtained by the IVIM is reliable for a larger interval. Furthermore, the solution by IVIM is still bounded and does not go to infinity as the solution given by the VIM. However, each subpopulation given by the IVIM starts to deviate from the RK-4 solution at about $t = 10$.

The solutions resulted from the fourth-iteration of MVIM and MIVIM for $t \in [0, 60]$ using $\Delta t = 3$ and $\Delta t = 2$ are respectively depicted in Figure 1 and Figure 2. Figure 1 shows that the solution given by the MVIM with $\Delta t = 3$ for subpopulation susceptible ($v(t)$) and subpopulation isolation ($y(t)$) have a very good agreement with the RK-4 solution. However, the MVIM solution for subpopulation exposed ($w(t)$) and subpopulation infected ($x(t)$) starts to deviate from the RK-4 solution at about $t = 2$; then it oscillates and finally converges to the RK-4 solution for larger t . Nonetheless, the MVIM solution with $\Delta t = 3$ has better performance than the VIM and IVIM solutions. The deviation of the MVIM solution is less pronounced for $\Delta t = 2$, see Figure 2. As expected, the MIVIM solution using either $\Delta t = 3$ or $\Delta t = 2$ for all subpopulations coincides with the RK-4 solution, which indicates that the MIVIM has significantly better performance than other methods (VIM, IVIM, and MVIM).

To further study the MVIM and MIVIM performance, we show in Table 2 the mean absolute error (MAE) of the solutions obtained by the fourth-iteration of VIM, IVIM, MVIM and MIVIM. The MAE is calculated by comparing the approximate solution with the RK-4 solution, which is evaluated on the same grid size $h = t_{i+1} - t_i, \forall i$. Here \mathcal{E}_v denotes the MAE of variable $v(t)$. The MAE of other variables is expressed in the same way. Table 2 shows that MVIM has better performance than VIM and IVIM. Among all the methods discussed above, MIVIM is the most effective method to solve the system (1). For the multistage method, smaller grid size (Δt) generally leads to a more accurate solution.

TABLE 2. Mean absolute error (MAE) of the solution obtained by the fourth-iteration of VIM, IVIM, MVIM and MIVIM.

MAE	VIM	IVIM	MVIM ($\Delta = 3$)	MVIM ($\Delta = 2$)	MIVIM ($\Delta = 3$)	MIVIM ($\Delta = 2$)
\mathcal{E}_v	5.508e+12	7.711e-02	9.746e-04	1.925e-04	4.623e-04	1.253e-04
\mathcal{E}_w	5.508e+12	3.551e-02	3.632e-03	4.323e-04	2.078e-04	5.632e-05
\mathcal{E}_x	1.635e+06	1.352e-02	3.528e-03	3.903e-04	1.419e-04	3.844e-05
\mathcal{E}_y	4.364e+05	2.596e-02	1.135e-03	8.917e-05	1.313e-04	3.532e-05

5. CONCLUSION

We have proposed two types of multistage variational method to solve the mathematical model of COVID-19 with isolation. The proposed methods are the multistage version of VIM and IVIM which have been recently introduced in the literature. The difference between the multistage VIM (MVIM) and the multistage IVIM (MIVIM) lies on the number of restricted variations included in the correction functional. The MIVIM has less number of restricted variations. In general, the multistage methods give more accurate solutions on much longer time intervals than the classical versions. Our numerical example demonstrates that the MIVIM has the best performance compared to VIM, IVIM and MVIM. The accuracy of solution of both MVIM and MIVIM can be increased by taking smaller subinterval (Δt) or by taking more number of iteration on each subinterval.

ACKNOWLEDGEMENTS

This research was funded by FMIPA-UB via PNBP-University of Brawijaya according to DIPA-UB No. DIPA-023.17.2.677512/2021 and Contract of Professor and Doctoral Research Grant No. 1584/UN10.F09/PN/2021.

CONFLICT OF INTERESTS

The authors declare that there is no conflict of interests.

REFERENCES

- [1] A.A. Agyeman, K.L. Chin, C.B. Landersdorfer, D. Liew, R. Ofori-Asenso, Smell and taste dysfunction in patients with COVID-19: A systematic review and meta-analysis, *Mayo Clinic Proc.* 95 (2020), 1621–1631. <https://doi.org/10.1016/j.mayocp.2020.05.030>.
- [2] K. Roosa, Y. Lee, R. Luo, A. Kirpich, R. Rothenberg, J.M. Hyman, P. Yan, G. Chowell, Short-term forecasts of the COVID-19 epidemic in Guangdong and Zhejiang, China: February 13–23, 2020, *J. Clin. Med.* 9 (2020), 596. <https://doi.org/10.3390/jcm9020596>.
- [3] K. Wu, D. Darcet, Q. Wang, D. Sornette, Generalized logistic growth modeling of the COVID-19 outbreak: comparing the dynamics in the 29 provinces in China and in the rest of the world, *Nonlinear Dyn.* 101 (2020), 1561–1581. <https://doi.org/10.1007/s11071-020-05862-6>.
- [4] I. Darti, A. Suryanto, H.S. Panigoro, H. Susanto, Forecasting COVID-19 epidemic in Spain and Italy using a generalized Richards model with quantified uncertainty, *Commun. Biomath. Sci.* 3 (2020), 90–100. <https://doi.org/10.5614/cbms.2020.3.2.1>.
- [5] I. Darti, U. Habibah, S. Astutik, W.M. Kusumawinahyu, Marsudi, A. Suryanto, Comparison of phenomenological growth models in predicting cumulative number of COVID-19 cases in East Java Province, Indonesia, *Commun. Math. Biol. Neurosci.* 2021 (2021), 14. <https://doi.org/10.28919/cmbn/5338>.
- [6] W.O. Kermack, A.G. McKendrick, A contribution to the mathematical theory of epidemics, *Proc. R. Soc. London.* 115(1927), 235-240. <https://doi.org/10.1098/rspa.1927.0118>.
- [7] A. Zeb, E. Alzahrani, V.S. Erturk, G. Zaman, Mathematical model for coronavirus disease 2019 (COVID-19) containing isolation class, *BioMed. Res. Int.* 2020 (2020), 3452402. <https://doi.org/10.1155/2020/3452402>.
- [8] O.D. Makinde, Adomian decomposition approach to a SIR epidemic model with constant vaccination strategy, *Appl. Math. Comput.* 184 (2007), 842–848. <https://doi.org/10.1016/j.amc.2006.06.074>.
- [9] A. Yıldırım, Y. Cherruault, Analytical approximate solution of a SIR epidemic model with constant vaccination strategy by homotopy perturbation method, *Kybernetes.* 38 (2009), 1566–1575. <https://doi.org/10.108/03684920910991540>.
- [10] J.-H. He, Homotopy perturbation technique, *Computer Meth. Appl. Mech. Eng.* 178 (1999), 257–262. [https://doi.org/10.1016/S0045-7825\(99\)00018-3](https://doi.org/10.1016/S0045-7825(99)00018-3).
- [11] A.R. Ghotbi, A. Barari, M. Omidvar, G. Domairry, Application of homotopy perturbation and variational iteration methods to SIR epidemic model, *J. Mech. Med. Biol.* 11 (2011), 149–161. <https://doi.org/10.1142/S0219519410003836>.
- [12] J.-H. He, Variational iteration method – a kind of non-linear analytical technique: some examples, *Int. J. Non-Linear Mech.* 34 (1999), 699–708. [https://doi.org/10.1016/S0020-7462\(98\)00048-1](https://doi.org/10.1016/S0020-7462(98)00048-1).

- [13] S. Mungkasi, Variational iteration and successive approximation methods for a SIR epidemic model with constant vaccination strategy, *Appl. Math. Model.* 90 (2021), 1–10. <https://doi.org/10.1016/j.apm.2020.08.058>.
- [14] Trisilowati, R.D. Hastuti, I. Darti, A. Suryanto, On the implementation of a variational iteration method for a SEIQR COVID-19 epidemic model, *Commun. Math. Biol. Neurosci.* 2021 (2021), 94. <https://doi.org/10.28919/cmbn/6848>.
- [15] B. Batiha, M. S. M. Noorani, I. Hashim, and E. S. Ismail, The multistage variational iteration method for a class of nonlinear system of ODEs, *Physica Scripta* 76(2007), 388. <https://doi.org/10.1088/0031-8949/76/4/018>.
- [16] F. Geng, Y. Lin, M. Cui, A piecewise variational iteration method for Ricatti differential equations, *Computers Math. Appl.* 58(2009), 2518-2522. <https://doi.org/10.1016/j.camwa.2009.03.063>.
- [17] S.M. Goh, M.S.M. Noorani, I. Hashim, Efficacy of variational iteration method for chaotic Genesio system – Classical and multistage approach, *Chaos Solitons Fractals.* 40 (2009), 2152–2159. <https://doi.org/10.1016/j.chaos.2007.10.003>.